

Resonant soft x-ray scattering studies of interface reconstructions in SrTiO₃/LaAlO₃ superlattices

H. Wadati,^{1,a)} D. G. Hawthorn,¹ J. Geck,¹ T. Higuchi,² Y. Hikita,² H. Y. Hwang,^{2,3} L. Fitting Kourkoutis,⁴ D. A. Muller,⁴ S.-W. Huang,⁵ D. J. Huang,⁵ H.-J. Lin,⁵ C. Schüßler-Langeheine,⁶ H.-H. Wu,^{5,6} E. Schierle,⁷ E. Weschke,⁷ N. J. C. Ingle,¹ and G. A. Sawatzky¹

¹Department of Physics and Astronomy and AMPEL, University of British Columbia, Vancouver, British Columbia V6T 1Z1, Canada

²Department of Advanced Materials Science, University of Tokyo, Kashiwa, Chiba 277-8561, Japan

³Japan Science and Technology Agency, Kawaguchi 332-0012, Japan

⁴School of Applied and Engineering Physics, Cornell University, Ithaca, New York 14853, USA

⁵National Synchrotron Radiation Research Center, Hsinchu 30076, Taiwan

⁶II. Physikalisches Institut, Universität zu Köln, Zùlpicher Straße 77, D-50937 Köln, Germany

⁷Helmholtz-Zentrum Berlin für Materialien und Energie, Albert-Einstein-Str. 15, D-12489 Berlin, Germany

(Received 3 July 2009; accepted 15 September 2009; published online 21 October 2009)

We present resonant soft x-ray scattering studies of Ti 3*d* and O 2*p* states at the interfaces of SrTiO₃/LaAlO₃ superlattices. From reflectivity analyses, focusing on the (003) peak which is forbidden for our “ideal” superlattice structure, we concluded that the LaO|TiO₂/SrO and the SrO|AlO₂/LaO interfaces have distinct reconstructions, breaking the heterostructure symmetry.

© 2009 American Institute of Physics. [doi:10.1063/1.3246788]

I. INTRODUCTION

Many oxide heteroepitaxial devices confront the need to manage different possible interface atomic configurations, which can have important effects on the electronic structure at the most electrically sensitive regions of the device. For example, in (001)-oriented manganite tunnel junctions or cuprate Josephson junctions, a perovskite such as SrTiO₃ (STO) is typically used as the insulating barrier. Because perovskites grow in unit cell (uc) blocks (a SrO/TiO₂ double layer for STO) in most growth techniques, the top and bottom interfaces across the barrier have different atomic terminations. Although most studies assume a symmetric barrier in these junctions neglecting this interface asymmetry, evidence is emerging that this is a crucial issue to understand and optimize.¹

One example of extremely anisotropic properties that arise as a function of interface termination is the interface between two band insulators STO and LaAlO₃ (LAO). This system is especially interesting due to the metallic conductivity² and even superconductivity³ found at the interface. In this STO/LAO heterostructure, the STO/LAO (SrO|AlO₂/LaO) interface is different from the LAO/STO (LaO|TiO₂/SrO) interface. The electronic structure of these interfaces has been studied both experimentally^{4–14} and theoretically,^{15–17} and there has been an intense debate about the origin of this metallicity; that is, whether it is due to oxygen vacancies (“extrinsic”)^{9,10} or due to the polar nature of the LAO structure,⁴ which could result in an “electronic reconstruction” as found in surfaces of polar materials by Hesper *et al.*¹⁸ Photoemission spectroscopy has been recently used to observe the electronic structures of such interfaces individually^{19–23} but it cannot be applied to the study of het-

erostructures with multiple interfaces due to its surface sensitivity. Therefore, little experimental information about the change in the electronic structure in multilayers incorporating both interfaces has been obtained.

In this study we investigated the electronic structure of the STO/LAO superlattice (SL) by resonant soft x-ray scattering,²⁴ which has recently been used to study LaMnO₃(LMO)/SrMnO₃(SMO) (Ref. 25) and La₂CuO₄/La_{1.64}Sr_{0.36}CuO₄ (Ref. 26) SLs. Since x-ray scattering is a photon-in photon-out process, resonant soft x-ray scattering is bulk sensitive, and can be applied to insulators as well as metals. In this sense, this technique is complementary to photoemission, and well suited for studying the electronic structure of multilayers nondestructively. While normal x-ray scattering is proportional to the number of electrons, that is the mass density of materials, in resonant x-ray scattering one can obtain the information on the electronic structures near the Fermi level,²⁷ which are composed of transition-metal 3*d* and oxygen 2*p* states, by tuning photon energies to the energy of transition-metal 2*p*→3*d* or oxygen 1*s*→2*p* absorption edges.

The (003) forbidden peak was used in Ref. 25 to study the electronic structure of symmetric interfaces in LMO/SMO. Here we show that a similar experimental approach can be used to differentially probe the asymmetry of interfaces in ABO₃/A'B'O₃ SLs, where two distinctly different interfaces are formed. We introduce a model which is used to analyze the energy dependence of the scattering in terms of the known energy dependence of the absorption of the parent bulk compounds, by taking into account the effects of the photon energy-dependent refraction, the finite thickness of the SL, which removes the total extinction in otherwise forbidden (003) reflections, and the photon energy-dependent absorption depth which again has an energy-dependent finite

^{a)}Electronic mail: wadati@phas.ubc.ca.

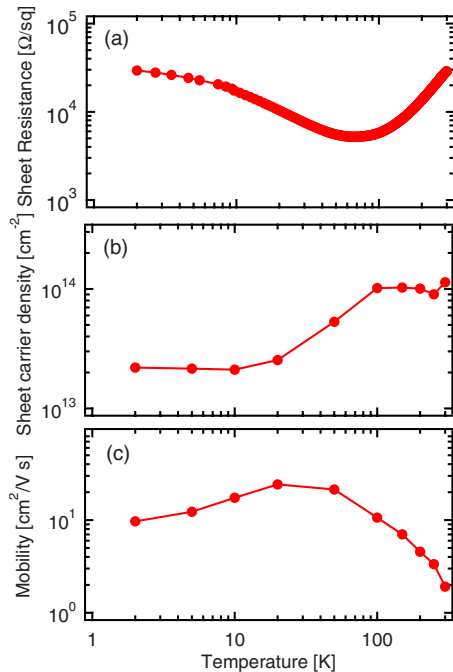


FIG. 1. (Color online) Transport properties of STO/LAO SL. (a) Sheet resistance, (b) sheet carrier density, (c) mobility.

size effect. From our study of the photon energy-dependent (002) and (003) Bragg peak positions and the overall reflectivity spectra, we obtained direct spectroscopic evidence for distinct reconstruction and electronic properties at the two types of interfaces in STO/LAO SLs. These results indicate that a simple SL of two components with asymmetric interface reconstructions is sufficient to strongly break inversion symmetry, without the requirement of three constituents as theoretically proposed²⁸ and experimentally realized.^{29–31}

II. EXPERIMENT

The SL sample consisted of seven periods of 12 ucs of STO and six ucs of LAO. The present samples were grown on a TiO_2 -terminated STO (001) substrate³² by pulsed laser deposition at an oxygen pressure of 1.0×10^{-5} Torr and a substrate temperature of 1073 K. Figure 1 shows the transport properties of the STO/LAO SL. The sheet resistance of the SL in Fig. 1(a) was about $10^4 \Omega/\text{sq}$, much larger than the case with significant oxygen vacancies.¹² There is an up-turn in sheet resistance at low temperatures. This behavior was also observed in a single interface of LAO/STO (Ref. 14) and was attributed to the decreased carrier number and mobility with decreasing temperature as shown in Figs. 1(b) and 1(c). The resonant soft x-ray scattering experiments were performed at the elliptically polarized-undulator beamline of NSRRC, Taiwan. The spectra were taken at 80 K. The incident light was polarized in the scattering plane (π polarization) with the detector integrating over both final polarizations, i.e., both the $\pi \rightarrow \sigma$ and $\pi \rightarrow \pi$ scattering channels. We also measured x-ray absorption spectroscopy (XAS) spectra in the fluorescence-yield mode.

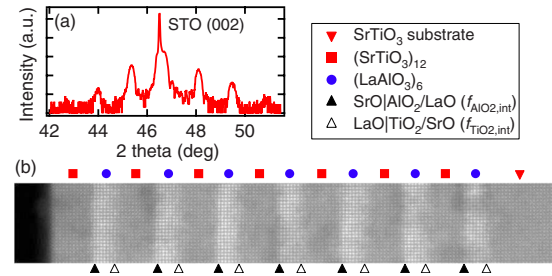


FIG. 2. (Color online) Characterization of the STO/LAO SL. (a) XRD pattern, (b) STEM image with scattering factors defined for the interfaces.

III. RESULTS AND DISCUSSION

Figure 2 shows the characterization of the STO/LAO SL by x-ray diffraction (XRD) (a) and scanning transmission electron microscopy (STEM) (b). From the XRD pattern shown in Fig. 2(a), one can see SL peaks and oscillations between these peaks. The lattice constant of one period of the SL was determined to be $73.45 \pm 0.03 \text{ \AA}$ from the peak positions of the SL peaks. The STEM image in Fig. 2(b) shows well-defined SL interfaces. There is more atomic interdiffusion in LaO|TiO₂/SrO interfaces than in SrO|AlO₂/LaO interfaces, consistent with the result reported in Ref. 4.

Figure 3 shows the x-ray reflectivity spectra measured at 455 eV (Ti 2*p* off-resonance) (a) and 458.4 eV (Ti 2*p* on-resonance) (b). The Ti 2*p* XAS spectrum is shown in the bottom panel of Fig. 4(a). There are four basic structures with dominant components corresponding to $2p_{3/2} \rightarrow t_{2g}$, $2p_{3/2} \rightarrow e_g$, $2p_{1/2} \rightarrow t_{2g}$, and $2p_{1/2} \rightarrow e_g$ transitions. The line shape is almost the same as that of bulk pure STO,³³ which means that the formal valence of Ti is close to 4+ in the SL, consistent with the recent report of the Ti 2*p* XAS spectra of a single interface of LAO/STO.¹³ Here we point out the following three points which show the advantage and necessity of resonant soft x-ray scattering over XAS. The first one is that XAS does not have any information of depth profile but just observes the average, so is not sensitive to the possible

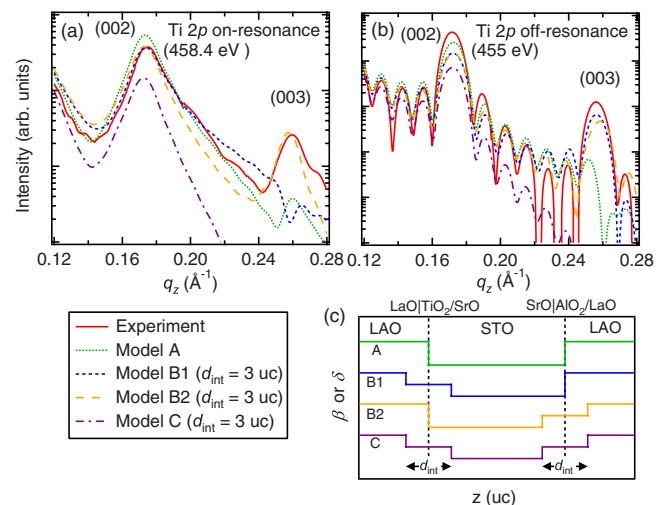


FIG. 3. (Color online) Comparison of the reflectivity spectra between experiment and calculation. (a) Ti 2*p* on-resonance, (b) Ti 2*p* off-resonance, (c) models of our SL samples.

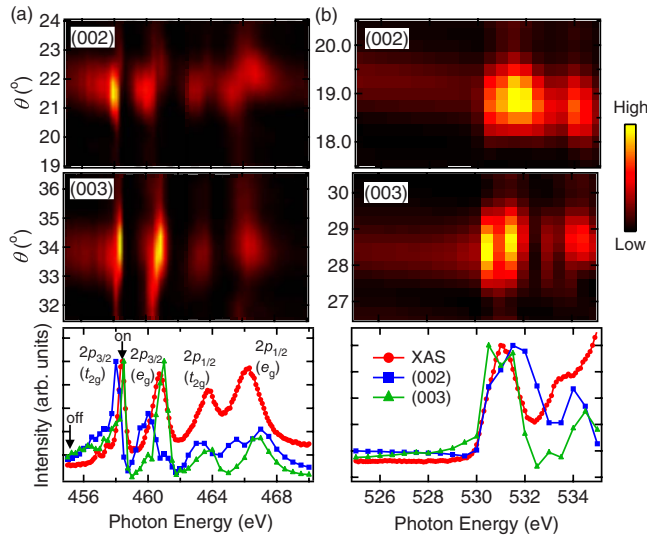


FIG. 4. (Color online) Photon-energy dependence of the (002) and (003) peaks near the Ti 2*p* (a) and O 1*s* (b) absorption edges. Top and middle panels show intensity maps of (002) and (003) regions, respectively. Here bright parts correspond to high intensities. Bottom panels show the (002) and (003) peak heights together with the XAS spectra.

existence of Ti³⁺ in the interface, which contributes to only a small amount of the total Ti 2*p* XAS spectrum. The second is that XAS measures only the imaginary part of dielectric constants, while scattering measures both real and imaginary parts, resulting in a phase in the scattering amplitude which is state dependent and causes strong interference effects in the scattering intensity. The final point is that XAS is not especially sensitive to interfaces and thus is not appropriate to study multilayers, while interface sensitivity can be achieved only by performing a scattering-type experiment, as is the main topic of the paper. The reflectivity spectra in Figs. 3(a) and 3(b) show finite-size Fresnel oscillations corresponding to the total thickness of seven periods, and (002) and (003) Bragg peaks. The oscillations are clear at off-resonance (b), but not evident at on-resonance (a). This is because the attenuation length of photons at 455 eV is about 100 nm, which is comparable to the total thickness when including the incident angle of about 20°–30°, but at 458.4 eV the attenuation length of only about 20 nm (Ref. 34) is much shorter than the total thickness and therefore the oscillations are not observed. Since the ratio of STO and LAO thicknesses are 2:1, the (003) peak would be forbidden in the infinitely thick and the zero absorption limit for samples of the ideal structure. The structure factors for (002) and (003) peaks are given as

$$\begin{aligned}
 S(002) &= f_{\text{TiO}_2, \text{int}} + (0.94 + 1.63i)f_{\text{TiO}_2, \text{bulk}} \\
 &\quad + (-0.50 + 0.87i)f_{\text{AlO}_2, \text{int}} + (-1.44 - 2.50i)f_{\text{AlO}_2, \text{bulk}} \\
 &\quad + (1.27 + 2.19i)(f_{\text{SrO}} - f_{\text{LaO}}), \\
 S(003) &= f_{\text{TiO}_2, \text{int}} - f_{\text{TiO}_2, \text{bulk}} + f_{\text{AlO}_2, \text{int}} - f_{\text{AlO}_2, \text{bulk}}, \quad (1)
 \end{aligned}$$

where $f_{\text{TiO}_2, \text{int}}$ and $f_{\text{AlO}_2, \text{int}}$ are the scattering factors at the interface as defined in Fig. 2(b), $f_{\text{TiO}_2, \text{bulk}}$ and $f_{\text{AlO}_2, \text{bulk}}$ are those for bulk structures (SrO/TiO₂/SrO and LaO/AlO₂/LaO), and f_{SrO} and f_{LaO} are those for SrO and

LaO layers, respectively. From Eq. (1) one can see that (002) is not particularly interface sensitive, but (003) is an interface-sensitive peak, which will be forbidden if the interface has the same scattering factor as bulk. In the case of LMO/SMO SL, the (003) peak was observed only on-resonance, but here it is observed in both on-resonance and off-resonance. We consider that this is due to the difference of the electronic structures between interface and bulk states ($f_{\text{TiO}_2, \text{bulk}} \neq f_{\text{TiO}_2, \text{int}}$, $f_{\text{AlO}_2, \text{bulk}} \neq f_{\text{AlO}_2, \text{int}}$), and/or atomic inter-diffusion, and lateral roughness at the interfaces. We now focus on a “normal Bragg” (002) peak, and a “forbidden interface-sensitive” (003) peak.

To analyze the reflectivity spectra in Figs. 3(a) and 3(b), we used the recursive Parratt’s method^{35,36} and simulated the reflectivity. Here we considered four models as shown in Fig. 3(c). Model A is the case where all interfaces are sharp. Model C is the case without any sharp interfaces with β or δ (here the refractive index n is equal to $1 - \delta + i\beta$) at the interface taken to be the average of that of STO and LAO. These two models are considered as “symmetric models” because they do not consider the difference of LaO|TiO₂/SrO and SrO|AlO₂/LaO interfaces. Asymmetric models are models B1 and B2. These models include different interfaces as far as the refractive index is concerned. In model B1, only the SrO|AlO₂/LaO interfaces are sharp and in model B2, only the LaO|TiO₂/SrO interfaces are sharp. It was previously reported that metallic behavior is only observed at LaO|TiO₂/SrO (Ref. 2) and also the LaO|TiO₂/SrO interfaces are atomically less sharp than the SrO|AlO₂/LaO,⁴ seeming to support model B1. Motivated by these studies, we investigated which model can best describe the reflectivity spectra. The comparison of the reflectivity spectra between experiment and calculation are shown in Figs. 3(a) and 3(b). One should note here that the energy dependence of the attenuation length of photons (i.e., on-resonance and off-resonance) has been taken into account by the energy dependence of the imaginary part of the refractive index β . From these figures one can see that the strong (003) peaks are only present in asymmetric models. In the two asymmetric models, model B1 reproduces the experimental results fairly well for Ti 2*p* off-resonance (b), but for Ti 2*p* on-resonance (a), model B2 gives a better description of the experiment. Also we obtain the best fitting when the thickness of the interface (d_{int}) is taken to be about 3 uc. We should note here that in model A, with no reconstruction, the (003) peak is still present at on-resonance in Fig. 3(a). This is due to the short penetration depth of the x rays at resonance, providing imperfect extinction as described before. From these results, we conclude that our SL is a highly asymmetric system with two different types of interfaces, and the thickness of the interface is about 3 uc, but we cannot conclude which model (B1 or B2) is better to describe the experiment. In all four models, the interfaces are assumed to be independent of depth, which is evidenced not to be the case from the STEM data in Fig. 2(b) and may explain why none of these models perfectly fits the experimental data. However, the fact that the intensity of the (002) peak relative to that of the

oscillations is well reproduced by models B1 and B2 means that the distribution in interface roughness is not a dominant factor.

Figure 4 shows the photon-energy dependence of the (002) and (003) peaks near the Ti 2*p* (a) and O 1*s* (b) absorption edges. From the top and middle panels one can see that both the (002) and (003) peaks show resonant enhancement at these edges. The bottom panels show the (002) and (003) peak heights together with the XAS spectra. These peaks show enhancement where the Ti 2*p* or O 1*s* absorption is strong. In O 1*s* there is no evidence of pre-edge structures from states in the band gap. This is in sharp contrast to the results of the LMO/SMO SL,²⁵ where a pre-edge feature appears corresponding to states at the Fermi level. This difference can be explained by the difference of the nature of metallicity. In the case of LMO/SMO, metallic behavior is due to the hole doping of insulating LMO, resulting in unoccupied states at the top of the valence band, whereas in the case of STO/LAO, metallicity is due to electron doping of insulating STO so no new unoccupied states appear that would be probed by resonant soft x-ray scattering. We should note here that the energy-dependent behaviors of the (002) and (003) peaks are very different, suggestive of some form of interfacial reconstruction.

Further evidence for electronic reconstruction at the interface is gleaned from an analysis of the peak positions at these absorption edges. In the normal Bragg's law $m\lambda = 2d \sin \theta$, where m is an integer, and d is the thickness of one uc of the SL. However, near the absorption edges, we must use the following modified Bragg's law,³⁷ which takes into account the effects of refraction

$$m\lambda = 2d \sin \theta \left(1 - \frac{4\bar{\delta}d^2}{m^2\lambda^2} \right). \quad (2)$$

Here the refractive index n is written as $n = 1 - \delta + i\beta$. For a system with ideally sharp interfaces between the two components, $\bar{\delta}$ is defined as the average of δ 's of STO and LAO, that is, $\bar{\delta} \approx 2\delta_{\text{STO}}/3 + \delta_{\text{LAO}}/3$. δ and β are related to the real and imaginary parts of the atomic scattering factors f_1^0 and f_2^0 , respectively. Since f_1^0 cannot be determined experimentally, we use the relationship that f_2^0 is proportional to absorption and determined f_2^0 from the XAS spectra normalized to the values from Henke's table.³⁸ f_1^0 is then obtained from the Kramers–Kronig transformation. The details of these procedures are described in Ref. 37.

Figure 5 shows the analyses of the (002) and (003) peak positions by using the calculated δ and Eq. (2). In the calculation, there is a large difference with finite δ , which indicates that the effects of refraction are substantial in these absorption edges. From panels (a) and (c), one can see that at the (002) peak (normal Bragg peak) the agreement between experiment and calculation is good, which confirms the validity of our analyses. However, panels (b) and (d) show that at the (003) peak (interface-sensitive peak) the agreement is rather poor. Our results are not a direct proof of the electronic reconstruction at the interface but it will be difficult to explain the disagreement by just assuming structure reconstruction without assuming any sort of electronic reconstruction

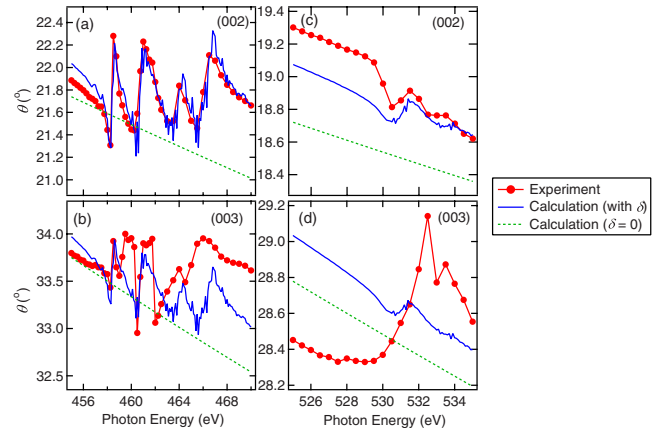


FIG. 5. (Color online) Peak-position analyses by considering the effects of refraction (δ). (a) (002) at the Ti 2*p* edge, (b) (003) at the Ti 2*p* edge, (c) (002) at the O 1*s* edge, (d) (003) at the O 1*s* edge.

tion effects (one possibility is changing the valence of Ti from 4+ to 3+ at the interface). A plausible explanation could be that the electronic reconstruction of Ti 3*d* and O 2*p* states at the interface changes the optical properties from those of the pure components. This reveals that the underlying assumption of electronically abrupt interfaces is not appropriate and implies a different electronic structure and therefore also a different energy-dependent dielectric constant from that assumed in Eq. (2). In order to distinguish, however, between electronic reconstruction and oxygen vacancies, we need a detailed theoretical understanding of the energy-dependent resonant scattering and the electronic structure of the interface. This is an important topic of our present-day research.

IV. CONCLUSION

In summary, we investigated the electronic structures of the STO/LAO SL by resonant soft x-ray scattering. The forbidden (003) peak was observed even at off-resonance, in sharp contrast to the case of LMO/SMO.²⁵ From reflectivity analyses, we found that the LaO|TiO₂/SrO and the SrO|AlO₂/LaO interfaces have quite different electronic structures, breaking the inversion symmetry of this two-component SL. From the peak position analyses taking into account the effects of refraction, we found spectroscopic evidence for electronic reconstruction of Ti 3*d* and O 2*p* states at the interface.

ACKNOWLEDGMENTS

The authors would like to thank I. Elifimov and A. Fujimori for informative discussions. H.W. acknowledges financial support from the Japan Society for the Promotion of Science. This work was supported by the DFG (J.G. and C.S.-L., the latter through Grant No. SFB 608) and was made possible by financial support from the Canadian funding Agencies NSERC, CRC, CIFAR, and CFI.

¹H. Yamada, Y. Ogawa, Y. Ishii, H. Sato, M. Kawasaki, H. Akoh, and Y. Tokura, *Science* **305**, 646 (2004).

²A. Ohtomo and H. Y. Hwang, *Nature (London)* **427**, 423 (2004).

³N. Reyren, S. Thiel, A. D. Caviglia, L. F. Kourkoutis, G. Hammer, C.

- Richter, C. W. Schneider, T. Kopp, A.-S. Ruetschi, D. Jaccard, M. Gabay, D. A. Muller, J.-M. Triscone, and J. Mannhart, *Science* **317**, 1196 (2007).
- ⁴N. Nakagawa, H. Y. Hwang, and D. A. Muller, *Nature Mater.* **5**, 204 (2006).
- ⁵M. Huijben, G. Rijnders, D. H. A. Blank, S. Bals, S. V. Aert, J. Verbeeck, G. V. Tendeloo, A. Brinkman, and H. Hilgkamp, *Nature Mater.* **5**, 556 (2006).
- ⁶S. Thiel, G. Hammerl, A. Schmehl, C. W. Schneider, and J. Mannhart, *Science* **313**, 1942 (2006).
- ⁷A. Brinkman, M. Huijben, M. V. Zalk, J. Huijben, U. Zeitler, J. C. Maan, W. G. V. D. Wiel, G. Rijnders, D. H. A. Blank, and H. Hilgkamp, *Nature Mater.* **6**, 493 (2007).
- ⁸G. Herranz, M. Basletic, M. Bibes, C. Carretero, E. Tafa, E. Jacquet, K. Bouzehouane, C. Deranlot, A. Hamzic, J.-M. Broto, A. Barthelemy, and A. Fert, *Phys. Rev. Lett.* **98**, 216803 (2007).
- ⁹W. Siemons, G. Koster, H. Yamamoto, W. A. Harrison, G. Lucovsky, T. H. Geballe, D. H. A. Blank, and M. R. Beasley, *Phys. Rev. Lett.* **98**, 196802 (2007).
- ¹⁰A. Kalabukhov, R. Gunnarsson, J. Borjesson, E. Olsson, T. Claeson, and D. Winkler, *Phys. Rev. B* **75**, 121404(R) (2007).
- ¹¹P. R. Willmott, S. A. Pauli, R. Herger, C. M. Schlepütz, D. Martoccia, B. D. Patterson, B. Delley, R. Clarke, D. Kumah, C. Cionca, and Y. Yacoby, *Phys. Rev. Lett.* **99**, 155502 (2007).
- ¹²M. Basletic, J.-L. Maurice, C. Carrétéro, G. Herranz, O. Copie, M. Bibes, É. Jacquet, K. Bouzehouane, S. Fusil, and A. Barthélémy, *Nature Mater.* **7**, 621 (2008).
- ¹³M. Salluzzo, J. C. Cezar, N. B. Brookes, V. Bisogni, G. M. De Luca, C. Richter, S. Thiel, J. Mannhart, M. Huijben, A. Brinkman, G. Rijnders, and G. Ghiringhelli, *Phys. Rev. Lett.* **102**, 166804 (2009).
- ¹⁴C. Bell, S. Harashima, Y. Hikita, and H. Y. Hwang, *Appl. Phys. Lett.* **94**, 222111 (2009).
- ¹⁵R. Pentcheva and W. E. Pickett, *Phys. Rev. B* **74**, 035112 (2006).
- ¹⁶M. S. Park, S. H. Rhim, and A. J. Freeman, *Phys. Rev. B* **74**, 205416 (2006).
- ¹⁷S. Ishibashi and K. Terakura, *J. Phys. Soc. Jpn.* **77**, 104706 (2008).
- ¹⁸R. Hesper, L. H. Tjeng, A. Heeres, and G. A. Sawatzky, *Phys. Rev. B* **62**, 16046 (2000).
- ¹⁹M. Takizawa, H. Wadati, K. Tanaka, M. Hashimoto, T. Yoshida, A. Fujimori, A. Chikamtsu, H. Kumigashira, M. Oshima, K. Shibuya, T. Mihara, T. Ohnishi, M. Lippmaa, M. Kawasaki, H. Koinuma, S. Okamoto, and A. J. Millis, *Phys. Rev. Lett.* **97**, 057601 (2006).
- ²⁰Y. Hotta, H. Wadati, A. Fujimori, T. Susaki, and H. Y. Hwang, *Appl. Phys. Lett.* **89**, 251916 (2006).
- ²¹H. Wadati, Y. Hotta, A. Fujimori, T. Susaki, H. Y. Hwang, Y. Takata, K. Horiba, M. Matsunami, S. Shin, M. Yabashi, K. Tamasaku, Y. Nishino, and T. Ishikawa, *Phys. Rev. B* **77**, 045122 (2008).
- ²²K. Yoshimatsu, R. Yasuhara, H. Kumigashira, and M. Oshima, *Phys. Rev. Lett.* **101**, 026802 (2008).
- ²³M. Takizawa, Y. Hotta, T. Susaki, Y. Ishida, H. Wadati, Y. Takata, K. Horiba, M. Matsunami, S. Shin, M. Yabashi, K. Tamasaku, N. Nishino, T. Ishikawa, A. Fujimori, and H. Y. Hwang, *Phys. Rev. Lett.* **102**, 236401 (2009).
- ²⁴P. Abbamonte, L. Venema, A. Rusydi, G. A. Sawatzky, G. Logvenov, and I. Bozovic, *Science* **297**, 581 (2002).
- ²⁵S. Smadici, P. Abbamonte, A. Bhattacharya, X. Zhai, A. Rusydi, J. N. Eckstein, S. D. Bader, and J.-M. Zuo, *Phys. Rev. Lett.* **99**, 196404 (2007).
- ²⁶S. Smadici, J. C. T. Lee, S. Wang, P. Abbamonte, A. Gozar, G. Logvenov, C. D. Cavellin, and I. Bozovic, *Phys. Rev. Lett.* **102**, 107004 (2009).
- ²⁷K. J. Thomas, J. P. Hill, S. Grenier, Y.-J. Kim, P. Abbamonte, L. Venema, A. Rusydi, Y. Tomioka, Y. Tokura, D. F. McMorro, G. Sawatzky, and M. van Veenendaal, *Phys. Rev. Lett.* **92**, 237204 (2004).
- ²⁸N. Sai, B. Meyer, and D. Vanderbilt, *Phys. Rev. Lett.* **84**, 5636 (2000).
- ²⁹M. P. Warusawithana, E. V. Colla, J. N. Eckstein, and M. B. Weissman, *Phys. Rev. Lett.* **90**, 036802 (2003).
- ³⁰Y. Ogawa, H. Yamada, T. Ogasawara, T. Arima, H. Okamoto, M. Kawasaki, and Y. Tokura, *Phys. Rev. Lett.* **90**, 217403 (2003).
- ³¹H. N. Lee, H. M. Christen, M. F. Chisholm, C. M. Rouleau, and D. H. Lowndes, *Nature (London)* **433**, 395 (2005).
- ³²M. Kawasaki, K. Takahashi, T. Maeda, R. Tsuchiya, M. Shinohara, O. Ishihara, T. Yonezawa, M. Yoshimoto, and H. Koinuma, *Science* **266**, 1540 (1994).
- ³³M. Abbate, F. M. de Groot, J. C. Fuggle, A. Fujimori, Y. Tokura, Y. Fujishima, O. Strebel, M. Domke, G. Kaindl, J. van Elp, B. T. Thole, G. A. Sawatzky, M. Sacchi, and N. Tsuda, *Phys. Rev. B* **44**, 5419 (1991).
- ³⁴J. Schlappa, C. Schuster-Langeheine, C. F. Chang, Z. Hu, E. Schierle, H. Ott, E. Weschke, G. Kaindl, M. Huijben, G. Rijnders, D. H. A. Blank, and L. H. Tjeng, e-print arXiv:0804.2461v1.
- ³⁵L. G. Parratt, *Phys. Rev.* **95**, 359 (1954).
- ³⁶J. H. Underwood and J. T. W. Barbee, *Appl. Opt.* **20**, 3027 (1981).
- ³⁷D. Attwood, *Soft X-Rays and Extreme Ultraviolet Radiation* (Cambridge University Press, Cambridge, 1999).
- ³⁸B. L. Henke, E. M. Gullikson, and J. C. Davis, *At. Data Nucl. Data Tables* **54**, 181 (1993).